

Effect of molecular architecture of *in situ* reactive compatibilizer on the morphology and interfacial activity of an immiscible polyolefin/polystyrene blend

Sanghyo Kim, Jin Kon Kim* and C. E. Park

Department of Chemical Engineering, Pohang University of Science and Technology,
 Pohang, Kyungbuk 790-784, Korea

(Received 3 August 1995; revised 5 February 1996)

Two different types of *in situ* compatibilizers, poly(ethylene-*ran*-acrylic acid) (PE-*r*-AA) and poly(propylene-*graft*-acrylic acid) (PP-*g*-AA), are added to the polystyrene/poly(styrene-*ran*-glycidyl methacrylate) (PS-GMA) system to study the effect of the distribution of functional units across the entire polymer chain (molecular architecture) of an *in situ* compatibilizer on the morphology and the reduction in domain size of the disperse phase. The acrylic acid group in both PE-*r*-AA and PP-*g*-AA is known to react very easily with the epoxy group in PS-GMA, and thus the PE (or PP)-*graft*-PS copolymer is formed. We have shown that a random-type copolymer of PE-*r*-AA is a very effective compatibilizer, in that the domain size of the disperse phase in the PE-*r*-AA/PS/PS-GMA blend was significantly reduced when increasing the amount of PS-GMA. However, a graft-type copolymer of PP-*g*-AA is *not* an effective compatibilizer to reduce domain size of the disperse phase in PP-*g*-AA/PS/PS-GMA blend even when PS-GMA is added up to 9 wt%. This result is explained by the existence of an inhomogeneous distribution of functional units of AA in PP-*g*-AA and the homopolymer poly(acrylic acid) (PAA), while for PE-*r*-AA functional units of AA are well distributed across the entire chain, and no homopolymer of PAA exists. The existence of an inhomogeneous distribution of functional units in PP-*g*-AA was studied by dynamic mechanical thermal analysis and by scanning electron microscopy or transmission electron microscopy. © 1997 Elsevier Science Ltd. All rights reserved.

(Keywords: compatibility; poly(ethylene-*ran*-acrylic acid); poly(propylene-*graft*-acrylic acid))

INTRODUCTION

Polymer blends often have a large interfacial tension and poor interfacial adhesion, and thus exhibit poor mechanical properties relative to their constituent components due to immiscibility between constituent components^{1–4}. The interfacial tension is usually related to the domain size of the dispersed phase, and the interfacial adhesion becomes very important in order to retain the morphology against high stress or strain^{3,4}.

In order to improve the mechanical properties of immiscible polymer blends, compatibilizers such as block copolymers and graft copolymers have been widely used, since block or graft copolymers are very effective in reducing the interfacial tension and improving interfacial adhesion by polymer chain entanglement or bridging at the interface^{5–12}. For example, the interfacial tension of a blend with a copolymer can be reduced to 40–70% of that of immiscible polymer blends when only 2 wt% of these copolymers is added^{5–8}. Fayt and co-workers^{9–11} have found that as a compatibilizer to improve mechanical properties, (i) a block copolymer is more effective than a graft copolymer, (ii) a diblock copolymer is more effective than a triblock or star-shaped copolymer, and (iii) a tapered-diblock copolymer is more effective than a pure-diblock copolymer.

However, there are some limits to the use of a block or a graft copolymer as a compatibilizer in immiscible polymer blends. One is the difficulty in adequately dispersing a block copolymer near the interface between two phases due to its high viscosity. Another difficulty to be expected is that an added block copolymer can localize in a homopolymer phase in a micelle form rather than at the interface^{13–15}. Recently, the use of a polymer having hydrogen bonding, ionic bonding and acid–base complex functional groups to improve miscibility of two immiscible polymer blends has been studied^{16–18}. However, these kinds of compatible blends show phase separation when the temperature is higher than the dissociation temperature¹⁹.

In order to overcome these disadvantages, reactive blending techniques in which *in situ* graft or block copolymers as compatibilizers are produced due to reaction between functional units in the polymer blends during melt blending have been proposed and developed^{20–23}. Certain functional units on the polymer chain of an *in situ* compatibilizer can react very easily with other functional units in one of the constituent components in an immiscible polymer blend. The functional unit(s) is easily introduced by a copolymerization reaction step or by the graft reaction during the extrusion process. For example, maleic anhydride polypropylene (and/or ethylene–propylene rubber), which is suitable as an *in situ* compatibilizer to make polypropylene/nylon alloys, is

* To whom correspondence should be addressed

usually made by the graft reaction during the extrusion process. Three pairs of reactive groups are presently used in industry: (i) anhydride/amine; (ii) carboxylic acid/epoxy; and (iii) oxazoline/anhydride or carboxylic acid^{21,22}.

It is quite natural to speculate that in addition to the number of functional units, the molecular architecture, that is, how functional units are distributed across the entire polymer chain, of *in situ* compatibilizers may significantly affect the final morphology, and thus mechanical properties of the polymer system. However, to the best of our knowledge, there is no report investigating the effect of the molecular architecture of *in situ* compatibilizers on the morphology and mechanical properties of polymer blends.

In this study we employ the reaction between carboxylic acid and epoxy groups existing in polymer chains in order to address this deficit. Note that the reaction between these two functional groups occurs very easily during melt mixing at higher temperatures^{24,25}. Specifically, poly(ethylene-*ran*-acrylic acid) (PE-*r*-AA) and poly(propylene-*graft*-acrylic acid) (PP-*g*-AA) were chosen to be used as *in situ* compatibilizers in the polystyrene/poly(styrene-*ran*-glycidyl methacrylate) (PS-GMA)/acrylic acid functionalized polyolefin system in order to investigate the effect of the molecular architecture of acrylic acid (AA), i.e. random type in PE-*r*-AA, and graft type in PP-*g*-AA, on the morphology and the change in domain size of the disperse phase.

EXPERIMENTAL

Materials

The polystyrene (PS) used in this study was a commercial grade (GPPS-G116) from the Dongbu Petrochemical Co., Korea. Its number-average molecular weight (M_n) and the polydispersity index (M_w/M_n) are 140 000 and 2.3, respectively, as determined by gel permeation chromatography (g.p.c.) using calibration curves for standard polystyrene.

The PE-*r*-AA was a commercial grade supplied by the Dow Chemical Co. under the trade mark Primacor 3150, having an M_n of 20 000 with a polydispersity of 8.7, determined by high-temperature g.p.c. (Waters 150C) using calibration curves for standard PE. The amount of acrylic acid in PE-*r*-AA was 3.0 wt%, determined by n.m.r. Thus, about 8.3 AA units per chain, based on the number-average molecular weight, are present.

The PP-*g*-AA was a commercial grade (Polybond 1002) from the Uniroyal Chemical Co. in pellet form having an M_n of 73 000 with a polydispersity of 2.5, determined by high-temperature g.p.c. (Waters 150C) using calibration curves for standard PE. The amount of AA in PP-*g*-AA was 8.0 wt%, determined by n.m.r. Thus, about 80 AA units per chain, based on the number-average molecular weight, are present if *all* the AA is assumed to be attached to the PP chain.

The PS-GMA employed in this study was kindly donated by the LG Chemical Co., Korea, and was prepared by suspension polymerization²⁵. The M_n and polydispersity index of PS-GMA are 46 000 and 2.5, respectively. The amount of GMA in PS-GMA is 2.0 wt%, determined by ¹³C n.m.r.²⁵. Thus, about 6.4 epoxy groups are present on each PS-GMA chain.

Melt blending

The materials as received were dried in a vacuum oven at 100°C for 1 day. The PE-*r*-AA (or PP-*g*-AA)/PS blends having two different blend ratios of 10/90 and 30/70 (w/w) were prepared using varying amounts of PS-GMA (0–10 wt% based on the total PS phase consisting of neat PS and PS-GMA) using an internal mixer (Brabender Plasticorder) at a speed of 50 r.p.m. The wall temperature inside the internal mixer was 200°C for PE-*r*-AA/PS blends and 210°C for PP-*g*-AA/PS blends.

Morphology

A scanning electron microscope (Jeol JSM-840A) was used to observe the morphology of specimens fractured at the cryogenic temperature, and then coated with a thin layer of gold. To determine the average particle size, Quantimet 570 image analysis (Cambridge Instruments) was used. About 200–300 particles were used to obtain the number-average particle size of each blend. To observe the possible existence of a phase-separate domain of poly(acrylic acid) (PAA) homopolymer in PP-*g*-AA, a transmission electron microscope (Jeol JEM 200CX) was used. The specimen was stained by osmium tetroxide (OsO₄) for 2.5 days. It should be mentioned that before staining PAA with OsO₄, pretreatment of the specimen by hydrazine for 3 days and drying it thoroughly for 3 days under vacuum was necessary to ensure good contrast between PAA and PP²⁶. When PAA could effectively be stained by OsO₄, it appeared dark on transmission electron microscopy (TEM).

Dynamic mechanical thermal property

In order to compare the dynamic storage and loss moduli (E' and E'') and the loss tangent ($\tan \delta$) of neat polypropylene with those of PP-*g*-AA, each sample was run in the single cantilever bending mode with a strain amplitude of 32 μm using a dynamic mechanical thermal analyser (model MK-11, Polymer Laboratories). Measurement was carried out from –50 to 150°C with a heating rate of 3°C min⁻¹.

Rheological measurement

In order to compare the viscosity ratio of PE-*r*-AA or PP-*g*-AA to neat PS, the complex viscosities (η^*) of neat PS, PE-*r*-AA and PP-*g*-AA at various angular frequencies (ω) were measured using a Rheometrics Dynamic Spectrometer (RDS II) using 25 mm circular discs in the oscillatory shear mode at 200 and 210°C.

RESULTS AND DISCUSSION

Morphologies

The change in number average particle size (D_n) of the dispersed phase of PE-*r*-AA in the 10/90 PE-*r*-AA/PS blend and that of the dispersed phase of PP-*g*-AA in the 10/90 PP-*g*-AA/PS blend with the amount of PS-GMA (weight per cent based on neat PS and PS-GMA) is given in *Figure 1*. Also, scanning electron micrograph (SEM) images are given in *Figure 2a* for 10/90 PE-*r*-AA/PS without PS-GMA (*Figure 2a-1*) and 10 wt% of PS-GMA (*Figure 2a-2*), and for 10/90 PP-*g*-AA/PS without PS-GMA (*Figure 2b-1*) and 10 wt% of PS-GMA (*Figure 2b-2*). Due to limitations of space, we have not shown all the obtained SEM images. Note that as described previously

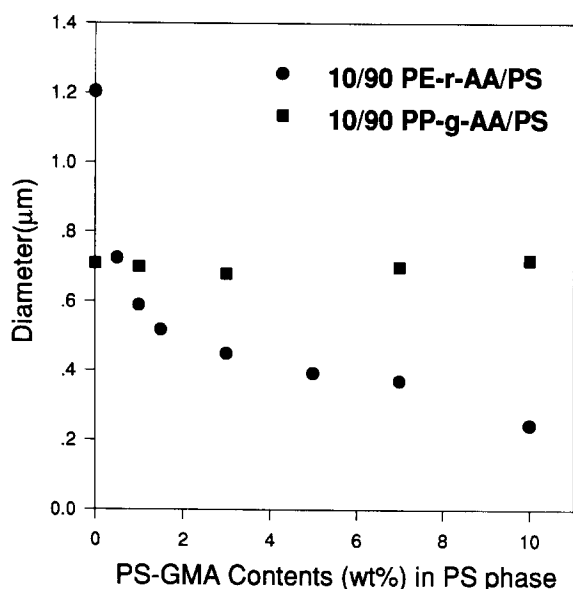


Figure 1 Plots of the number-average diameter of the dispersed phase versus the amount of PS-GMA (weight per cent based on neat PS and PS-GMA) for two different blend systems: 10/90 PE-*r*-AA/PS (●) and 10/90 PP-*g*-AA/PS (■)

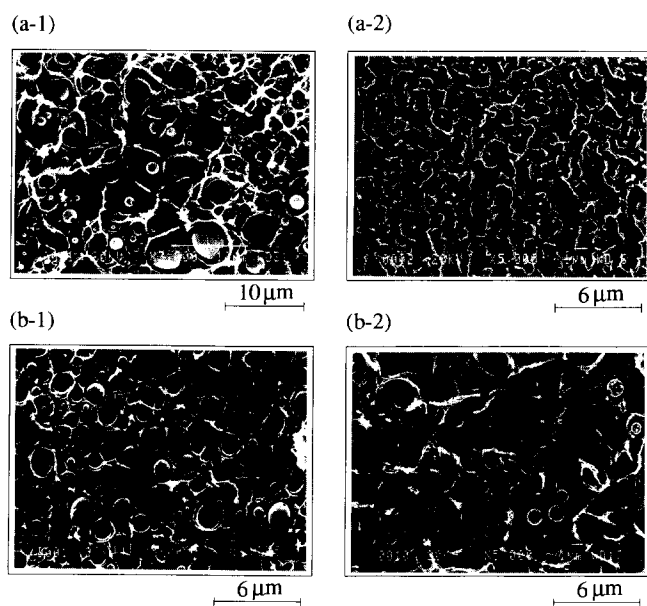


Figure 2 SEM images for two different blend systems with different amounts of PS-GMA: (a-1) 10/90/0 PE-*r*-AA/PS/PS-GMA, (a-2) 10/81/9 PE-*r*-AA/PS/PS-GMA; (b-1) 10/90/0 PP-*g*-AA/PS/PS-GMA, (b-2) 10/81/9 PP-*g*-AA/PS/PS-GMA

in the Experimental section, the setting temperature of the internal mixer was 200°C for the PE-*r*-AA/PS blend and 210°C for the PP-*g*-AA/PS blend. It can be seen in Figures 1 and 2 that D_n of PE-*r*-AA in the PE-*r*-AA/PS blend is larger than that of PP-*g*-AA in the PP-*g*-AA/PS blend when PS-GMA was not added to either blend. It is known that the domain size of the disperse phase in two immiscible polymer blends prepared by melt blending depends mainly on three factors: (i) the viscosity and elasticity ratio of the disperse phase to the continuous phase; (ii) the interaction parameter between the constituent components; and (iii) the magnitude of the applied shear stress or shear rate²⁷. Since the applied

shear rate is almost the same for the two blend systems due to using the same mixing speed in the internal mixer, we consider two other effects.

The complex viscosity (η^*) ratio of PE-*r*-AA to neat PS at 200°C was 0.054 at 0.1 rad s⁻¹ and 0.132 at 17.5 rad s⁻¹, while the viscosity of PP-*g*-AA to neat PS at 210°C was 0.048 at 0.1 rad s⁻¹ and 0.128 at 17.5 rad s⁻¹. Since the average shear rate in the internal mixer employed in this study was about 17.5 rad s⁻¹²⁵, the difference in the viscosity ratio of the disperse phase to the continuous phase between the two blend systems is too small to explain the large difference in D_n of the two blend systems. Note that the disperse domain may increase with increasing elasticity of the dispersed phase. Since the elasticity of PE is usually larger than PP, this may explain in part the above result. However, we do not think that the elasticity difference is the major source of the large difference in D_n of the two blend systems.

Now, we consider the interaction parameter between PE-*r*-AA and PS and that between PP-*g*-AA and PS. It is well established that as the interaction parameter between constituent components becomes smaller, the better is the miscibility, and thus the smaller are the domain sizes of the disperse phase. In the context of mean-field theory, the effective interaction energy, Λ_{eff} of copolymer and homopolymer is given by^{28,29}:

$$\Lambda_{\text{eff}} = \phi_1 \Lambda_{1-S} + (1 - \phi_1) \Lambda_{AA-S} - \phi_1 (1 - \phi_1) \Lambda_{1-AA} \quad (1)$$

where '1' is either PE or PP, ϕ_1 is the volume fraction of PE or PP in PE-*r*-AA or PP-*g*-AA, and Λ_{ij} is the interaction energy between two monomers i and j which equals to $(\chi_{ij}/V_{\text{ref}})RT$, where χ_{ij} is the Flory interaction parameter, V_{ref} is the reference volume, R is the gas constant and T is the absolute temperature.

Since Λ_{ij} is not available in the literature at this present time, we estimate these values from solubility parameters due to Hildebrand³⁰:

$$\Lambda_{ij} = (\delta_i - \delta_j)^2 \quad (2)$$

where δ_i and δ_j are the solubility parameters of components i and j , respectively. Although the values of δ vary widely from one reference to another, in this study we estimate that the values of δ of PS, PE, PP and PAA to be 18.7, 15.1, 15.7 and 24.9 (Jcm⁻³)^{0.5}, respectively, as calculated by the group contributions method³¹. Substituting these values of δ_i and equation (2) into equation (1), Λ_{eff} was calculated to be 10.7 Jcm⁻³ for the PE-*r*-AA/PS blend and 5.27 Jcm⁻³ for the PP-*g*-AA/PS blend. It is very gratifying to find that the effective interaction energy for the former blend is twice that of the latter blend although PP-*g*-AA is not a random copolymer and many possible uncertainties are incurred in estimating the solubility parameter. It should be mentioned that within the context of mean-field theory the effective interaction energy of a blend containing an A-*ran*-B copolymer is equal to that of A-*graft*-B and A-*block*-B copolymers when the volume fraction of A in three copolymers is the same³²⁻³⁴. Based on the above analysis, we can conclude that the main reason that the domain size of the disperse phase in the PP-*g*-AA/PS blend is smaller than that in the PE-*r*-AA/PS blend might be due to the smaller value of the effective interaction energy of the former blend compared to that of the latter blend.

It should also be noted in Figures 1 and 2 that the D_{avg} of the dispersed phase of PE-*r*-AA in the 10/90

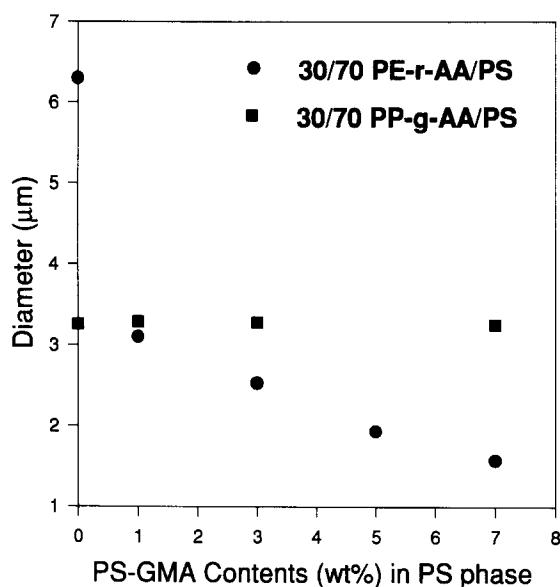


Figure 3 Plots of the number-average diameter of the dispersed phase versus the amount of PS-GMA for two different blend systems: 30/70 PE-r-AA/PS (●) and 30/70 PP-g-AA/PS (■)

PE-r-AA/PS blend decreases significantly until about 2 wt% of PS-GMA then decreases rather slowly with increasing amounts of PS-GMA. However, the D_n of the dispersed phase of PP-g-AA in 10/90 PP-g-AA/PS does not decrease at all even when the amount of PS-GMA is increased up to 10 wt% of the PS phase (i.e. 9 wt% of the total blend).

Figure 3 gives the plots of the number average particle size (D_n) of the dispersed phase of PE-r-AA in the 30/70 PE-r-AA/PS blend and that of the dispersed phase of PP-g-AA in 30/70 PP-g-AA/PS with the amount of PS-GMA. It can be seen in Figure 3 that (i) with increasing amounts of PS-GMA the D_n of the dispersed phase of PE-r-AA in the 30/70 PE-r-AA/PS blend decreases significantly until about 3 wt% of PS-GMA then decreases rather slowly, while the D_n of the dispersed phase of PP-g-AA in 30/70 PP-g-AA/PS does not decrease at all even when the amount of PS-GMA is increased up to 7 wt%, and (ii) the D_n of PE-r-AA in the PE-r-AA/PS blend is much larger than that of PP-g-AA in the PP-g-AA/PS blend when PS-GMA is not present in either blend, which are the same results as shown in Figure 1.

The results of Figures 1–3 lead us to conclude that PP-g-AA does not play a role as an effective *in situ* compatibilizer for the PP-g-AA/PS/PS-GMA blend system, while PE-r-AA does act as an *in situ* compatibilizer for the PE-r-AA/PS/PS-GMA blend system even if the number of available functional units of carboxylic acid in the PP-g-AA is greater than that in PE-r-AA.

The question then arises of why PP-g-AA does not play a role as an effective *in situ* compatibilizer while PE-r-AA does. First, it may be that the reaction between AA in PP-g-AA and the epoxy functional unit in PS-GMA does not occur sufficiently, thus producing only a small amount of PP-g-PS copolymer, while much PE-g-PS copolymer is formed due to an efficient reaction between AA in PE-r-AA and the epoxy unit in PS-GMA.

Figure 4 gives the torque change with blending time for the two blend systems, namely the 70/30 PP-g-AA/PS-GMA blend and the 70/30 PE-r-AA/PS-GMA blend,

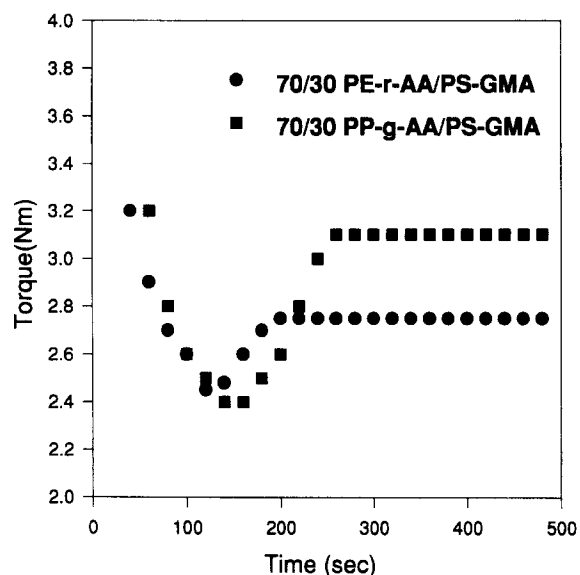


Figure 4 Torque change with time at the setting temperature of 200°C for two different blend systems: 70/30 PE-r-AA/PS-GMA (●) and 70/30 PP-g-AA/PS-GMA (■)

measured at a wall temperature of 200°C. It is seen that torque increment (plateau torque appearing after 5 min minus minimum torque appearing at 2 min) for 70/30 PP-g-AA/PS-GMA is greater than that of the 70/30 PE-r-AA/PS-GMA blend. Thus, we conclude that more reaction between PP-g-AA and PS-GMA occurs than between PE-r-AA and PS-GMA. The large increment in torque during melt blending for PP-g-AA/PS-GMA compared to PE-r-AA/PS-GMA is partially explained, since (i) the amount of reactive AA groups in PP-g-AA is greater than that in PE-r-AA, and (ii) PP-g-AA has a higher molecular weight than PE-r-AA. Note that torque is proportional to viscosity of the blend²⁵, thus the greater the molecular weight of the graft copolymer, the larger is the torque.

In order to investigate the amount of PP-g-PS copolymer formed from the 70/30 PP-g-AA/PS-GMA blend and that of PE-g-PS from the 70/30 PE-r-AA/PS-GMA blend, FT i.r. spectroscopy (Shimadzu; Model FT-IR 4300) was performed on powders of both blends before and after extraction by acetone at 50°C for 2 days. Note that unreacted PS-GMA in both blends could be extracted efficiently by acetone when both blends are ground into very fine powders in a liquid nitrogen environment.

It should be mentioned that the amounts of graft copolymer formed in this study were not easily investigated by size exclusion chromatography (s.e.c.). Since all polymers employed in this study have a very broad molecular distribution, the s.e.c. chromatogram for one polymer significantly overlapped the chromatograms of the other polymers; thus, we could not differentiate the characteristic peak corresponding to the graft copolymer formed during reaction. Of course, s.e.c. would be a very powerful technique with which to determine the amount of graft or block copolymer formed during reaction when the constituent components in blends have a very narrow molecular weight distribution²⁴.

When we employed the FT i.r. technique, we chose a wavenumber (ν) of 698 cm^{-1} , which corresponds to the absorption peak of =CH₂– in the aromatic ring, as the

characteristic ν for PS. Also, $\nu = 1468 \text{ cm}^{-1}$, corresponding to $-\text{CH}_2-$ in PE-*r*-AA, and $\nu = 1377 \text{ cm}^{-1}$, corresponding to $-\text{CH}_3$ in PP-*g*-AA, were chosen as the characteristic wavenumbers for PE-*r*-AA and PP-*g*-AA, respectively. The amount of unreacted PS-GMA in a blend could be obtained by the ratio of the absorption peak height between two characteristic wavenumbers for that blend before and after extraction. For instance, the ratio of the peak height of $\nu = 698 \text{ cm}^{-1}$ to either $\nu = 1468 \text{ cm}^{-1}$ for the PE blend or $\nu = 1377 \text{ cm}^{-1}$ for the PP blend after extraction was less than that for the respective blend without extraction. Using this FTi.r. technique, we found that the amount of unreacted PS-GMA in both blends was approximately the same, $\sim 10 \text{ wt}\%$ of the original amount of PS-GMA in both blends. Further, note that when the extracted portion was weighed after evaporating acetone, it was $\sim 3 \text{ wt}\%$ of the original weight of the blend, thus $\sim 10 \text{ wt}\%$ of the original amount of PS-GMA in the blend. Based on FTi.r. results and Figure 4, we can conclude that the reaction between AA in PP-*g*-AA and the epoxy functional unit in PS-GMA occurred sufficiently.

Morphologies of the fracture surface for the 70/30 PP-*g*-AA/PS-GMA blend and the 70/30 PE-*r*-AA/PS-GMA blend prepared by the Brabender internal mixer at 200°C are given in Figure 5. It can be seen in Figure 5 that distinct phase-separated domains are not visible in this magnification scale for the 70/30 PE-*r*-AA/PS-GMA blend, but that the domain size of the disperse phase for the 70/30 PP-*g*-AA/PS-GMA blend was $2\text{--}3 \mu\text{m}$ size. The domain size of the disperse phase for the 70/30 PP-*g*-AA/PS-GMA blend is very close to that for the 30/70 PP-*g*-AA/PS blend (see Figure 3), which means that the

disperse domain size for PP-*g*-AA/PS/PS-GMA blends changes very little, if at all, even if PS-GMA is added in amounts up to 30 wt%. However, we note from Figure 5b that for the 70/30 PP-*g*-AA/PS-GMA blend slightly improved interfacial adhesion between the disperse phase and the continuous phase can be expected since the disperse domain does not have a sharp interface.

Inhomogeneous distribution of acrylic acid in PP-*g*-AA

From Figures 3–5 we note that even if the reaction between AA in PP-*g*-AA and the epoxy group in PS-GMA occurs, the disperse domain size does not change very much, while the disperse domain size for PE-*r*-AA/PS-GMA decreases significantly. This result can be explained if there exists an inhomogeneous distribution of the AA functional group in the PP-*g*-AA chain, as a phase-separated domain, while a uniform distribution of AA in the PE-*r*-AA chain is expected. Note that PE-*r*-AA is synthesized by adding AA comonomer in a low-density PE (LDPE) synthesis process; thus, it is assumed that the AA units are well distributed across the entire chain. However, PP-*g*-AA is produced by a reactive extrusion process in an extruder where a radical initiator and AA monomer are added to the molten PP. Thus, a homopolymer of PAA can also be produced in addition to forming PP-*g*-AA copolymer. Once the PAA homopolymer is produced, it forms a phase-separated domain in the matrix of PP or PP-*g*-AA because the interaction parameter between PP and PAA is very large.

In order to check whether the phase-separated domain consisting of the PAA component really exists or not, we employed a selective solvent extraction method. Here, methanol was used as the solvent, since methanol dissolves PAA but not PP or PP-*g*-AA. Thus, any free PAA chains not grafted to PP chains in PP-*g*-AA will be solubilized into the methanol. An as received sample of PP-*g*-AA was cut into very thin slices to increase the surface area, to make its solubilization easier. The FTi.r. spectrum of the film prepared by drying the methanol solution was found to be essentially the same as the i.r. spectrum of pure PAA; for example, a peak at $\nu = 3600 \text{ cm}^{-1}$ (representing the OH group) and a peak at $\nu = 1730 \text{ cm}^{-1}$ (representing C=O) could be clearly seen.

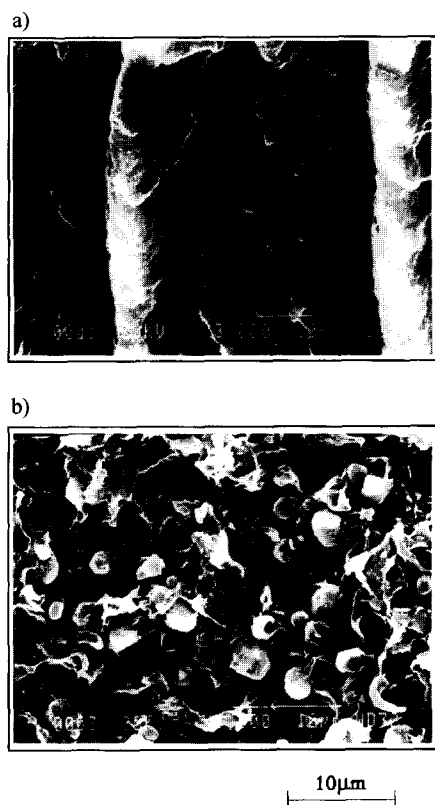


Figure 5 SEM images of fractured surfaces for two different blend systems: (a) 70/30 PE-*r*-AA/PS-GMA and (b) 70/30 PP-*g*-AA/PS-GMA

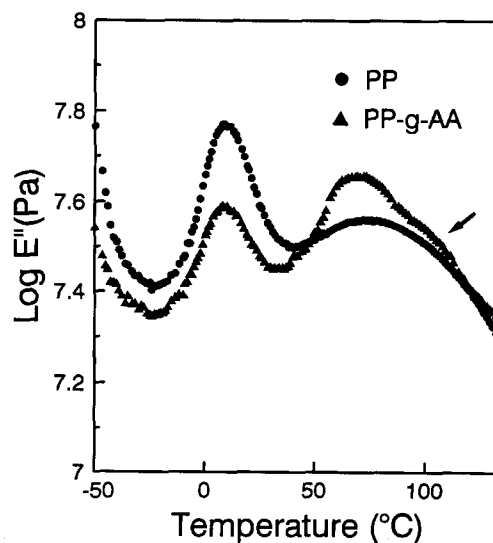


Figure 6 Plots of the dynamic loss modulus (E'') versus temperature for the homopolymer PP (●) and PP-*g*-AA (▲)

The existence of a phase-separated PAA domain in PP-g-AA could also be manifested by plots of the dynamic loss modulus (E'') versus temperature for pure PP and PP-g-AA (Figure 6). It is seen that (i) the characteristic β transition of PP, namely the glass transition, T_g , of the amorphous resin of PP, was found at about 0°C, and (ii) the transition generally recognized to be associated with the crystalline region of PP occurs at about 70–80°C for both components³⁵. However, in PP-g-AA a peak in E'' , although broad, appearing at around 110°C (marked by an arrow in Figure 6) is seen, and this is essentially the same as the glass transition, T_g , of the homopolymer PAA³⁶. It is now well established that the domain size must be at least 20 nm to observe the glass transition corresponding to the disperse phase in a blend measured by dynamic mechanical thermal analysis (d.m.t.a.) or d.s.c.³⁷. Therefore, from Figure 6 we consider that a phase-separated domain having a size of at least 20 nm exists in PP-g-AA.

SEM images of the fractured surface cut at cryogenic temperatures are given in Figure 7a for PE-r-AA, and in Figure 7b for PP-g-AA, in which distinct phase-separated domains having a size of 0.2–0.8 μm are clearly seen for PP-g-AA, while there are no signs of a phase-separated morphology in PE-r-AA.

In order to further determine the domain size of phase-separated PAA in PP-g-AA, TEM was used (Figure 8). Note that PAA can be stained by OsO₄ when pretreated with hydrazine, and appears dark. Various domain sizes ranging from 40 nm to 0.35 μm are clearly seen. However, phase-separated domains are not well distributed, i.e. a relatively high number of domains are visible in some regions while almost no domains are seen in other regions. Further, note that although we do not

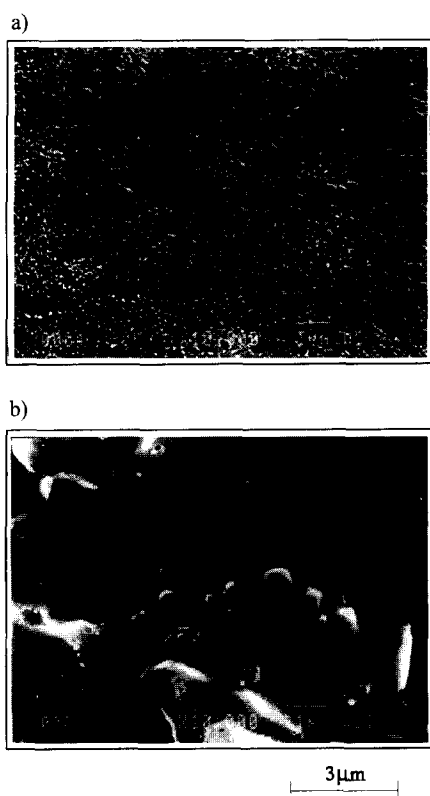


Figure 7 SEM images of fractured surfaces for two different copolymers: (a) PE-r-AA and (b) PP-g-AA

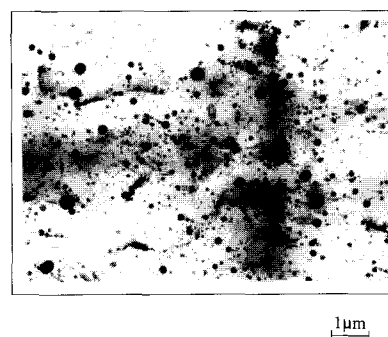


Figure 8 TEM image of an as-received PP-g-AA sample pretreated with hydrazine for 3 days followed by staining with OsO₄. Dark regions represent dispersed phases consisting of the PAA homopolymer

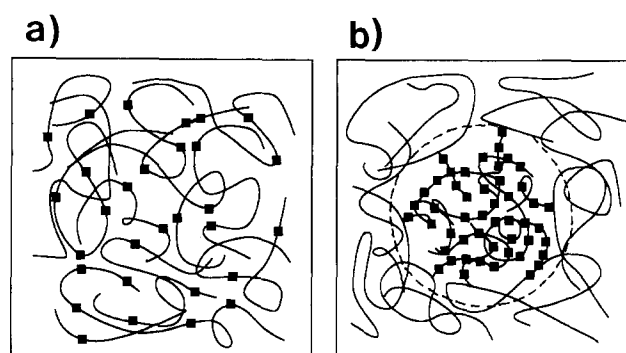


Figure 9 Schematic diagram of the distribution of AA (i.e. the molecular architecture) in two different copolymers: (a) PE-r-AA; and (b) PP-g-AA. ■, AA functional units

present a TEM image for PE-r-AA here, we could not see any phase-separated domains even when a magnification as high as $\times 200\,000$ was used.

It can be concluded from Figures 7 and 8 that the distribution of AA in PE-r-AA is quite different from that in PP-g-AA. It should be mentioned that if whole AA groups (8 wt%) had been grafted at only a single point in the PP main chain, the domain size of AA would have been much less than 20 nm when the end-to-end distance is considered. Thus, there is no choice but to assume that the large phase-separated domain having a size of $\sim 0.35 \mu\text{m}$ consists of many chains of homopolymer PAA and/or locally concentrated AA groups in the PP chain.

Finally, based on the above results we propose the schematic molecular architecture of PE-r-AA and PP-g-AA as shown in Figure 9. The AA units in PE-r-AA are well distributed across the entire chain, and thus the graft reaction between PE-r-AA and PS-GMA occurs uniformly along the chain, giving rise to a significant decrease in the domain size. However, because the AA units in PP-g-AA exist at very limited positions, and are not well distributed, the reaction between PP-g-AA and PS-GMA is highly constrained at certain places, and thus the graft copolymer has no ability to reduce the domain size.

This suggests to us that when a functional group such as AA is introduced into a polymer chain using a radical reaction during an extrusion process, extreme care must be taken in order to make an effective *in situ* compatibilizer. This means that one must choose a functional monomer incapable of polymerization by itself. One

good candidate for this purpose is the maleic anhydride functional unit. Note that when maleic anhydride is attached to a polymer using a radical initiator chain during an extrusion process, one does not have to consider the inhomogeneity, in contrast to PP-*g*-AA, because homopolymerization of maleic anhydride by the radical reaction is very difficult³⁸. Thus, there are many commercially available polymer alloys with a maleic anhydride modified polymer, for example polyolefin-*graft*-maleic anhydride (or poly(2,6 dimethyl 1,4-phenylene ether)-*graft*-maleic anhydride: PPE-*g*-MAH) is known to be an excellent *in situ* compatibilizer of polyolefins/nylon (or PPE/nylon) alloys which have good interfacial adhesion and mechanical properties^{23,39–41}.

CONCLUDING REMARKS

In this study we have shown that the molecular architecture of an *in situ* compatibilizer profoundly influenced the morphology and the reduction in domain size of the disperse phase in immiscible polyolefin and polystyrene blends. Specifically, a random-type copolymer of PE-*r*-AA acts as an effective compatibilizer in that the domain size of the disperse phase in a PE-*r*-AA/PS/PS-GMA blend was significantly reduced with increasing amounts of PS-GMA, while a graft-type copolymer of PP-*g*-AA does not do so in a PP-*g*-AA/PS/PS-GMA blend since there is no reduction in domain size of the disperse phase even when PS-GMA is added in amounts up to 9 wt%.

This result was explained by the existence of an inhomogeneous distribution of AA functional units in PP-*g*-AA and the PAA homopolymer. However, for PE-*r*-AA, AA functional units are well distributed across the entire chain and there is no PAA homopolymer. The existence of separated PAA homopolymer in PP-*g*-AA was confirmed by i.r. spectroscopy, and by a glass transition corresponding to homopolymer PAA as measured by d.m.t.a. Also, an inhomogeneous distribution of functional units in PP-*g*-AA could be demonstrated by a distinct phase-separated domain size of about 0.04–0.35 μm measured by SEM and TEM. Therefore, unless the functional units are well distributed across the entire chain, the better interfacial activity expected by reducing the domain size due to a graft copolymer formed during melt mixing will not occur even if sufficient functional units are present in the polymer chain and reaction between the two functional groups occurs easily. A study of the interfacial activity of PP-*g*-AA containing no PAA homopolymer, prepared by a selective solvent technique, on a PP-*g*-AA/PS-GMA blend will give us more insight on the effect of different molecular architectures on the compatibilization of two incompatible polymer blends of PP-*g*-AA/PS-GMA and PE-*r*-AA/PS-GMA, and is in progress in our laboratory.

ACKNOWLEDGEMENT

This work was supported in part by Functional Polymer ERC governed by KOSEF.

REFERENCES

- Folkes, M. J. and Hope, P. S. 'Polymer Blends and Alloys', Blackie, London, 1993
- Utracki, L. A. 'Polymer Alloys and Blends', Hanser, New York, 1989
- Tang, T. and Huang, B. *Polymer* 1994, **35**, 281
- Lee, Y. and Char, K. *Macromolecules* 1994, **27**, 2603
- Patterson, H. T., Hu, K. H. and Grindstaff, T. H. *J. Polym. Sci., C* 1971, **34**, 31
- Gaillard, P., Ossensbach, M. and Reiss, G. *Makromol. Chem., Rapid Commun.* 1980, **1**, 771
- Brown, H. R. *Macromolecules* 1989, **22**, 2859
- Anastasiadis, S. H., Gancarz, I. and Koberstein, J. T. *Macromolecules* 1989, **22**, 1449
- Fayt, R., Jerome, R. and Teyssie, Ph. *J. Polym. Sci., Polym. Lett. Ed.* 1981, **19**, 79
- Fayt, R., Jerome, R. and Teyssie, Ph. *J. Polym. Sci., Polym. Phys. Ed.* 1982, **20**, 2209
- Fayt, R., Jerome, R. and Teyssie, Ph. *J. Polym. Sci., Polym. Phys. Ed.* 1989, **27**, 775
- Creton, C., Kramer, E. J. and Hadziioannou, G. *Macromolecules* 1991, **24**, 1846
- Shull, K. *Macromolecules* 1993, **26**, 2346
- Whitmore, M. D. and Noolandi, J. *Macromolecules* 1985, **18**, 657
- Roe, R. J. *Macromolecules* 1986, **19**, 731
- Painter, P. C., Park, Y. and Coleman, M. M. *Macromolecules* 1989, **22**, 570
- Rutkowska, M. and Eisenberg, A. *Macromolecules* 1984, **17**, 821
- Moskala, E. J., Howe, S. E., Painter, P. C. and Coleman, M. M. *Macromolecules* 1984, **17**, 1671
- Russell, T. P., Jerome, R., Charlier, P. and Foucart, M. *Macromolecules* 1988, **21**, 1709
- Favis, B. D. *Can. J. Chem. Eng.* 1991, **69**, 619
- Xanthos, M. *Polym. Eng. Sci.* 1988, **28**, 1392
- Xanthos, M. and Dagli, S. S. *Polym. Eng. Sci.* 1991, **31**, 929
- Ide, F. and Hasegawa, A. *J. Appl. Polym. Sci.* 1974, **18**, 963
- Guegan, P., Macosko, C. W., Ishizone, T., Hirao, A. and Nakahama, S. *Macromolecules* 1994, **27**, 4993
- Kim, J. K. and Lee, H. *Polymer* 1996, **37**, 305
- Kanig, G. *Proc. Colloid Polym. Sci.* 1975, **57**, 176
- Han, C. D. 'Multiphase Flow in Polymer Processing', Academic Press, New York, Ch. 4, 1981
- Paul, D. J. and Barlow, J. W. *Polymer* 1984, **25**, 487
- Ten Brinke, G., Karasz, F. E. and MacKnight, W. J. *Macromolecules* 1983, **16**, 1827
- Van Krevelen, D. W. and Hoftyzer, P. J. 'Properties of Polymers', Elsevier, New York, Ch. 7, 1976
- Bicerano, J. 'Prediction of Polymer Properties', Marcel Dekker, New York, 1993
- Leibler, L. *Macromolecules* 1981, **13**, 1602
- Kim, J. K., Kimishima, K. and Hashimoto, T. *Macromolecules* 1993, **26**, 125
- Kim, J. K. *Polymer* 1995, **36**, 1243
- Liang, Z. and Williams, H. L. *J. Appl. Polym. Sci.* 1992, **44**, 699
- Brandrup, J. and Immergut, E. H. 'Polymer Handbook', Wiley, New York, 1975, Ch. 3
- Han, C. D. and Kim, J. K. *Polymer* 1993, **34**, 2533
- Gaylor, N. G., Metha, R., Mohan, D. R. and Kumar, V. *J. Appl. Polym. Sci.* 1992, **44**, 1941
- Han, C. D. and Chuang, K. *J. Appl. Polym. Sci.* 1985, **30**, 2431
- Ueno, K. and Maruyama, T. USP 4 315 086 (Sumitomo Chem. Co.), 1982
- Campbell, J. R., Hobbs, S. Y., Shea, T. J. and Watkins, V. H. *Polym. Eng. Sci.* 1990, **30**, 1056